

## Synthesis of Red-emitting (Gd, Ca, Eu)<sub>2</sub>W<sub>2</sub>O<sub>9</sub> Phosphors

Sun Woog Kim, Toshiyuki Masui, and Nobuhito Imanaka\*

Department of Applied Chemistry, Faculty of Engineering, Osaka University, 2-1 Yamadaoka, Suita, Osaka 565-0871

(Received February 10, 2011; CL-110118; E-mail: imanaka@chem.eng.osaka-u.ac.jp)

Red-emitting (Gd<sub>1-x-y</sub>Ca<sub>x</sub>Eu<sub>y</sub>)<sub>2</sub>W<sub>2</sub>O<sub>9-x</sub> phosphors (0 ≤ x ≤ 0.05, 0.05 ≤ y ≤ 1.00) were synthesized in a single phase form by conventional solid-state reaction. These phosphors exhibited excellent luminescent efficiency at excitation wavelengths of 394 and 464 nm, and the emission intensities were successfully enhanced by Ca<sup>2+</sup> doping into the Gd<sub>2</sub>W<sub>2</sub>O<sub>9</sub> lattice. The highest red emission intensity was obtained for (Gd<sub>0.58</sub>Ca<sub>0.02</sub>Eu<sub>0.40</sub>)<sub>2</sub>W<sub>2</sub>O<sub>8.98</sub>, and the emission intensities of this phosphor under excitations at 394 and 464 nm were 15.2 and 29.1 times higher, respectively, than those of a commercial (Y<sub>0.98</sub>Eu<sub>0.02</sub>)<sub>2</sub>O<sub>2</sub>S phosphor.

White light-emitting diodes (white LEDs) have been widely applied in displays and lamps as an alternative to conventional incandescent and fluorescent lamps. White LEDs of high chromatic purity can be fabricated from yellow-, green-, and red-emitting phosphors excited by a GaN-based blue chip or blue-, green-, and red-emitting phosphors excited by an InGaN LED chip in the near UV-region. However, the red-emitting phosphors are based on nitride and oxynitride, which are hard to synthesize in a single phase form. Therefore, investigations have been devoted to the search for new red-emitting materials based on oxide, which can show high luminescent efficiency under blue-light and near-UV irradiation.

Rare earth tungstates and alkaline rare earth tungstates have been widely investigated as a host material for phosphors, and tungstate phosphors can show good luminescent efficiency due to effective energy transfer from their tungstate groups to activator ions.<sup>1</sup> In particular, Eu<sup>3+</sup>-doped rare earth tungstates and alkali rare earth tungstates, (R, Eu)<sub>2</sub>W<sub>3</sub>O<sub>12</sub> and M(R, Eu)-W<sub>2</sub>O<sub>8</sub> (M: alkali metals and R: rare earths), exhibit good luminescent efficiency as red-emitting phosphors for use in white LEDs. These phosphors show strong optical absorption at 395 and 465 nm, corresponding to the emission wavelengths of GaN- and InGaN-based LED chips, respectively. However, the luminescent efficiency of the conventional tungstate phosphors mentioned above remains too low compared to those of green- and blue-emitting phosphors for use in white LEDs.<sup>2</sup>

In this study, on the other hand, we have focused on monoclinic gadolinium tungstate, Gd<sub>2</sub>W<sub>2</sub>O<sub>9</sub>, as a host material for the phosphor to realize a novel red-emitting phosphor with a high luminescent efficiency. In the series of rare earth tungstates, monoclinic Gd<sub>2</sub>W<sub>2</sub>O<sub>9</sub> has a suitable layer structure to act as a host material for phosphors, in which the GdO<sub>9</sub> polyhedral layers are separated by WO<sub>6</sub> octahedral layers in the direction of the *b* axis.<sup>3</sup> It was demonstrated in our previous studies that phosphors based on such a layered structure can show good photoluminescent properties.<sup>4</sup> It is well known that the luminescent properties of phosphors strongly depend on the interactions between activators in the host lattice. When the activator content is excessive, the emission intensity generally

decreases due to concentration quenching, because the decrease in the mean activator-activator distance often induces non-radiative deactivation. In a layered structure, however, energy transfer from one excited luminescent ion to another across the anion groups is inhibited by the long distance between the rare earth ions. Therefore, phosphors based on this layered structure should be resistant to concentration quenching.<sup>5</sup> In this study, red-emitting (Gd<sub>1-y</sub>Eu<sub>y</sub>)<sub>2</sub>W<sub>2</sub>O<sub>9</sub> phosphors were synthesized, and the photoluminescent properties were characterized. Furthermore, partial substitution of the Gd<sup>3+</sup> site with Ca<sup>2+</sup> was also carried out to enhance the emission intensity.

A mixture of Gd<sub>2</sub>O<sub>3</sub>, Eu<sub>2</sub>O<sub>3</sub>, CaO, and WO<sub>3</sub> was ground using a mortar, in which the amount of Eu<sup>3+</sup> was adjusted between 5 and 100% and the Ca<sup>2+</sup> content was varied from 0 to 5%. Then the mixture was mechanically ground using a planetary ball-milling apparatus (Pulverisette 7, FRITSCHE GmbH) for 3 h. The homogenous mixture was first calcined at 800 °C for 15 h and then calcined twice at 1000 °C for 15 h in air. After these calcinations, the samples were reground in a mortar and heated again at 1100 °C for 15 h in air.

The samples were characterized by X-ray powder diffraction (XRD; Rigaku Multiflex), X-ray fluorescence spectroscopy (XRF; Rigaku ZSX-100e), and scanning electron microscopy (SEM; Shimadzu SS-550). Photoluminescence (PL) excitation and emission spectra were recorded with a spectrofluorophotometer (Shimadzu RF-5300PC). The relative emission intensities of the samples were estimated by comparing the integrated area of the emission peak at 612 nm with that of a commercial (Y<sub>0.98</sub>Eu<sub>0.02</sub>)<sub>2</sub>O<sub>2</sub>S phosphor. The internal quantum yields were measured on a spectrofluorometer (Jasco FP-6500) with fluorescence integrate sphere unit (Jasco ISF-513). The experimental details are given in the Supporting Information.<sup>6</sup>

X-ray powder diffraction (XRD) patterns of the (Gd<sub>1-y</sub>Eu<sub>y</sub>)<sub>2</sub>W<sub>2</sub>O<sub>9</sub> (x = 0) phosphors were in good agreement with a single phase of highly crystalline monoclinic rare earth tungstate. The excitation spectrum of Eu<sup>3+</sup> emission at 612 nm for a (Gd<sub>0.65</sub>Eu<sub>0.35</sub>)<sub>2</sub>W<sub>2</sub>O<sub>9</sub> phosphor is shown in Figure 1. The excitation spectrum of the sample consisted of two broad bands from 250 to 360 nm, which correspond to charge-transfer (CT) transitions of Eu<sup>3+</sup>-O<sup>2-</sup> and O<sup>2-</sup>-W<sup>6+</sup>. Several strong narrow peaks were observed between 360 and 500 nm and were attributed to the f-f transitions of the Eu<sup>3+</sup> ion. Among these, the dominant sharp peaks at 394 and 464 nm corresponded to the <sup>7</sup>F<sub>0-5</sub>L<sub>6</sub> and the <sup>7</sup>F<sub>0-5</sub>D<sub>2</sub> transitions of Eu<sup>3+</sup>, respectively.<sup>1</sup> Generally, in Eu<sup>3+</sup>-doped red-emitting phosphors, the peak intensity of the CT transition is stronger than that of the f-f transitions, because the former is a spin-allowed transition and the latter is a forbidden transition. However, in tungstate phosphors, the CT transition intensity of Eu<sup>3+</sup>-O<sup>2-</sup> was relatively weak in the excitation spectrum, because the contribution of the O<sup>2-</sup>-W<sup>6+</sup> transition to the excitation was large.<sup>7</sup>

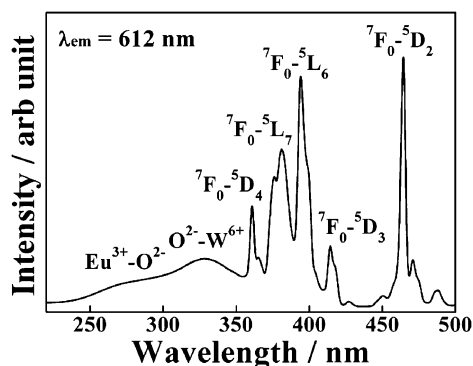


**Figure 1.** Excitation spectrum of the  $(\text{Gd}_{0.65}\text{Eu}_{0.35})_2\text{W}_2\text{O}_9$  phosphor.

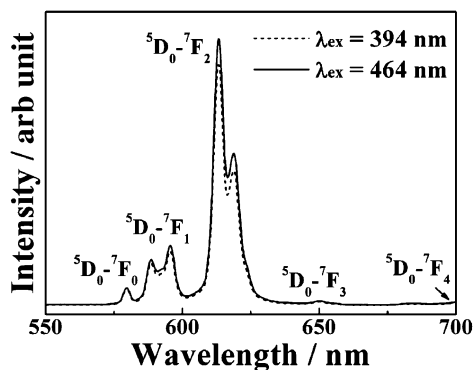
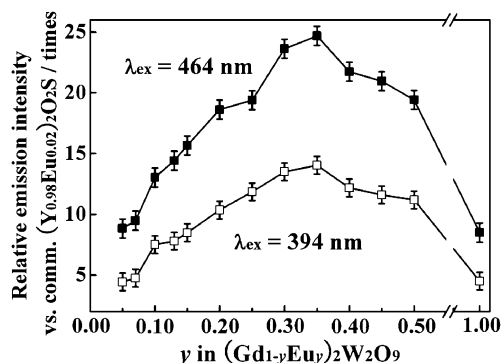


**Figure 2.** Emission spectra of the  $(\text{Gd}_{0.65}\text{Eu}_{0.35})_2\text{W}_2\text{O}_9$  phosphor.

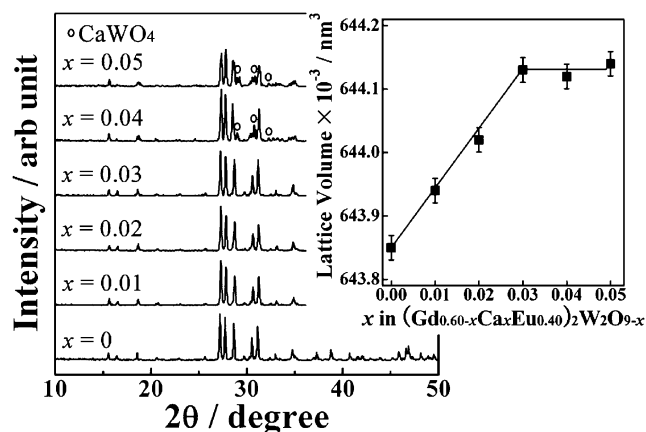
Figure 2 shows the emission spectra of a  $(\text{Gd}_{0.65}\text{Eu}_{0.35})_2\text{W}_2\text{O}_9$  phosphor with excitation at 394 and 464 nm. All emission peaks corresponded to the transition from the  $^5\text{D}_0$  excited level to the  $^7\text{F}_J$  ( $J = 0, 1, 2, 3,$  and  $4$ ) ground levels of  $\text{Eu}^{3+}$ . In the emission spectrum, the peak corresponding to the  $^5\text{D}_0\text{-}^7\text{F}_2$  electric dipole transition at 612 nm was more prominent than those of the  $^5\text{D}_0\text{-}^7\text{F}_1$  magnetic dipole transitions at 586 and 595 nm. This indicates that the  $\text{Eu}^{3+}$  ion occupies the  $\text{Gd}^{3+}$  ion site with no inversion symmetry. Therefore, the crystal structure of  $\text{Gd}_2\text{W}_2\text{O}_9$  makes it a suitable host material for red-emitting phosphors, because the ideal emission for a rich red color is a narrow band around 610 nm.

Figure 3 depicts the dependence of the emission intensity on the  $\text{Eu}^{3+}$  concentration in the  $(\text{Gd}_{1-y}\text{Eu}_y)_2\text{W}_2\text{O}_9$  ( $0.05 \leq y \leq 1.00$ ) phosphors. The maximum emission intensity was obtained for  $(\text{Gd}_{0.65}\text{Eu}_{0.35})_2\text{W}_2\text{O}_9$ , for which the emission intensities were 14.0 and 24.7 times higher than those of a commercial  $(\text{Y}_{0.98}\text{Eu}_{0.02})_2\text{O}_2\text{S}$  phosphor under excitation at wavelengths of 394 and 464 nm, respectively.

To enhance the emission intensity of the  $(\text{Gd}_{1-y}\text{Eu}_y)_2\text{W}_2\text{O}_9$  phosphor,  $\text{Ca}^{2+}$  was doped into the  $\text{Gd}_2\text{W}_2\text{O}_9$  host lattice. However, an impurity phase corresponding to tetragonal scheelite  $\text{CaWO}_4$  was observed in the samples with  $0.05 \leq y \leq 0.35$ , even if a nominal amount of Ca ( $x = 0.01$ ) was doped in  $(\text{Gd}_{1-x-y}\text{Ca}_x\text{Eu}_y)_2\text{W}_2\text{O}_{9-x}$ . As a result, the emission intensities became smaller than those of the samples without the  $\text{Ca}^{2+}$  doping. In contrast, for the samples with  $0.40 \leq y \leq 1.00$ , a



**Figure 3.** Dependence of the emission intensity on the  $\text{Eu}^{3+}$  concentration in the  $(\text{Gd}_{1-y}\text{Eu}_y)_2\text{W}_2\text{O}_9$  ( $0.05 \leq y \leq 1.00$ ) phosphors. The excitation wavelengths were 394 and 464 nm, and each relative emission intensity was evaluated by comparing the integrated area of the emission peak at 612 nm with that of a commercial  $(\text{Y}_{0.98}\text{Eu}_{0.02})_2\text{O}_2\text{S}$  phosphor.



**Figure 4.** XRD patterns of the  $(\text{Gd}_{0.60-x}\text{Ca}_x\text{Eu}_{0.40})_2\text{W}_2\text{O}_{9-x}$  ( $0 \leq x \leq 0.05$ ) phosphors. The inset shows compositional dependence of the lattice volume of the monoclinic  $\text{R}_2\text{W}_2\text{O}_9$  (R: rare earths) phase for the  $(\text{Gd}_{0.60-x}\text{Ca}_x\text{Eu}_{0.40})_2\text{W}_2\text{O}_{9-x}$  phosphors.

single phase corresponding to the monoclinic  $\text{R}_2\text{W}_2\text{O}_9$  (R: rare earths) structure was obtained, and the most significant enhancement of the emission intensity was observed in the sample with  $y = 0.40$ . Therefore, the  $\text{Eu}^{3+}$  concentration in the  $(\text{Gd}_{1-x-y}\text{Ca}_x\text{Eu}_y)_2\text{W}_2\text{O}_{9-x}$  phosphors was fixed to be  $y = 0.40$ .

Figure 4 shows the XRD patterns of the  $(\text{Gd}_{0.60-x}\text{Ca}_x\text{Eu}_{0.40})_2\text{W}_2\text{O}_{9-x}$  ( $0 \leq x \leq 0.05$ ) phosphors. It was clear that a single phase of the monoclinic rare earth tungstate structure was successfully obtained for the samples with  $x \leq 0.03$ , while a secondary phase of  $\text{CaWO}_4$  appeared for the solids with  $0.04 \leq x$ . Furthermore, the lattice volume of the monoclinic  $\text{R}_2\text{W}_2\text{O}_9$  phase in the prepared samples linearly increased with increasing  $x$  in the single phase region ( $x \leq 0.03$ ) as depicted in the inset, because the ionic radius of  $\text{Ca}^{2+}$  (0.1180 nm for 9 coordination)<sup>8</sup> is larger than that of  $\text{Gd}^{3+}$  (0.1107 nm for 9 coordination).<sup>8</sup> Since the lattice volume of the monoclinic  $\text{R}_2\text{W}_2\text{O}_9$  phase became constant in the two-phase mixture region ( $0.03 < x \leq 0.05$ ), it was clear that the solid solubility limit composition forming the single phase of the monoclinic

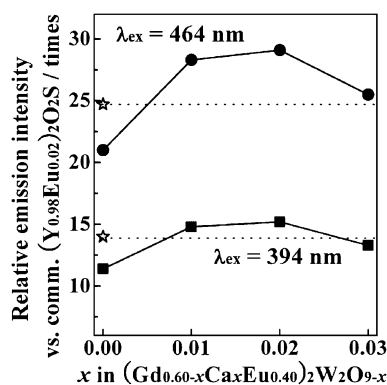


**Figure 5.** Dependence of the emission intensities on the  $\text{Ca}^{2+}$  concentration in the  $(\text{Gd}_{0.60-x}\text{Ca}_x\text{Eu}_{0.40})_2\text{W}_2\text{O}_{9-x}$  ( $0 \leq x \leq 0.03$ ) phosphors. The emission intensities of  $(\text{Gd}_{0.65}\text{Eu}_{0.35})_2\text{W}_2\text{O}_9$  ( $\star$ ) for excitations at 394 and 464 nm are also plotted for comparison.

$\text{R}_2\text{W}_2\text{O}_9$  structure is  $x = 0.03$  in  $(\text{Gd}_{0.60-x}\text{Ca}_x\text{Eu}_{0.40})_2\text{W}_2\text{O}_{9-x}$ . In addition, anion vacancies have to be produced within the lattice to maintain charge compensation, because  $\text{Ca}^{2+}$  has lower valence (divalent) than  $\text{Gd}^{3+}$  (trivalent).

The dependence of the emission intensities on the  $\text{Ca}^{2+}$  concentration in the  $(\text{Gd}_{0.60-x}\text{Ca}_x\text{Eu}_{0.40})_2\text{W}_2\text{O}_{9-x}$  ( $0 \leq x \leq 0.03$ ) phosphors is shown in Figure 5. The luminescent emission intensity was successfully enhanced by the  $\text{Ca}^{2+}$  doping, and the emission reached the maximum intensity at  $x = 0.02$  in  $(\text{Gd}_{0.60-x}\text{Ca}_x\text{Eu}_{0.40})_2\text{W}_2\text{O}_{9-x}$ . The increase of the emission intensity can be attributed to the decrease of electronegativity of the host rare earth cation. Since the electronegativity of  $\text{Ca}^{2+}$  (1.00)<sup>9</sup> is smaller than that of  $\text{Gd}^{3+}$  (1.20),<sup>9</sup> partial substitution of the  $\text{Gd}^{3+}$  site with  $\text{Ca}^{2+}$  results in the decrease in the electron attractive force of the rare earth ions. As a result, the charge-transfer efficiency from  $\text{O}^{2-}$  to  $\text{W}^{6+}$  is increased to enhance the peak intensity of the  $\text{Eu}^{3+}$  f–f transitions.<sup>7</sup> In addition, it has also been suggested that oxide anion vacancies might act as a sensitizer for the energy transfer to the rare earth ion due to the strong mixing of charge-transfer state (CTS).<sup>10</sup> On the other hand, the emission intensity tended to decrease with increasing the  $\text{Ca}^{2+}$  content beyond the optimum concentration, probably due to the excessive distortion in the host  $\text{Gd}_2\text{W}_2\text{O}_9$  lattice, which leads to fluorescence quenching.<sup>11</sup> The ionic radius of  $\text{Ca}^{2+}$  is larger than that of  $\text{Gd}^{3+}$ , so that the excess  $\text{Ca}^{2+}$  doping should introduce extra strain into the host  $\text{Gd}_2\text{W}_2\text{O}_9$  lattice. Therefore, emission quenching is expected beyond the optimum  $\text{Ca}^{2+}$  concentration.

Consequently, the maximum emission intensity was obtained for  $(\text{Gd}_{0.58}\text{Ca}_{0.02}\text{Eu}_{0.40})_2\text{W}_2\text{O}_{8.98}$ , and the  $\text{Ca}^{2+}$  concentration dependence of the emission intensity followed the same tendency for excitations at both 394 and 464 nm. The emission intensities of  $(\text{Gd}_{0.58}\text{Ca}_{0.02}\text{Eu}_{0.40})_2\text{W}_2\text{O}_{8.98}$  were 15.2 and 29.1 times higher than those of a commercial  $(\text{Y}_{0.98}\text{Eu}_{0.02})_2\text{O}_2\text{S}$  phosphor under the excitation wavelengths of 394 and 464 nm, respectively. The internal quantum efficiencies of  $(\text{Gd}_{0.58}\text{Ca}_{0.02}\text{Eu}_{0.40})_2\text{W}_2\text{O}_{8.98}$  at the excitation wavelength of 394 and 464 nm are estimated to be 58.6% and 49.7%, respectively. In addition, the emission intensities of  $(\text{Gd}_{0.58}\text{Ca}_{0.02}\text{Eu}_{0.40})_2\text{W}_2\text{O}_{8.98}$  were considerably higher than any yet reported for conventional phosphors based on rare earth tungstates or alkali rare earth

tungstates. The maximum emission intensity to date was obtained for  $\text{NaY}_{0.95}\text{Eu}_{0.05}(\text{WO}_4)(\text{MoO}_4)$  and was 7.28 times higher than that of  $(\text{Y}_{0.98}\text{Eu}_{0.02})_2\text{O}_2\text{S}$  for excitation at 393 nm.<sup>2,12</sup>

From the SEM observations, it is obvious that the particle size of  $(\text{Gd}_{0.58}\text{Ca}_{0.02}\text{Eu}_{0.40})_2\text{W}_2\text{O}_{8.98}$  is appreciably smaller than that of  $(\text{Y}_{0.98}\text{Eu}_{0.02})_2\text{O}_2\text{S}$ , and both of them have a granular particle morphology (Figure S1 in the Supporting Information).<sup>6</sup> The average particle sizes of  $(\text{Gd}_{0.58}\text{Ca}_{0.02}\text{Eu}_{0.40})_2\text{W}_2\text{O}_{8.98}$  and  $(\text{Y}_{0.98}\text{Eu}_{0.02})_2\text{O}_2\text{S}$  estimated from their size distribution (Figure S2) are 2.9 and 5.0  $\mu\text{m}$ , respectively.<sup>6</sup>

In summary, red-emitting phosphors based on gadolinium calcium tungstate,  $(\text{Gd}_{1-x-y}\text{Ca}_x\text{Eu}_y)_2\text{W}_2\text{O}_{9-x}$ , were synthesized in a single phase form by a conventional solid-state reaction. These phosphors were excited efficiently under excitations at 394 and 464 nm, and the photoluminescent emission intensity was effectively enhanced by the  $\text{Ca}^{2+}$  doping into the host  $(\text{Gd}_{0.60}\text{Eu}_{0.40})_2\text{W}_2\text{O}_9$  lattice. The maximum emission intensity was obtained for  $(\text{Gd}_{0.58}\text{Ca}_{0.02}\text{Eu}_{0.40})_2\text{W}_2\text{O}_{8.98}$ . The emission intensities of this phosphor were 15.2 and 29.1 times higher than those of a commercial  $(\text{Y}_{0.98}\text{Eu}_{0.02})_2\text{O}_2\text{S}$  phosphor under excitation at wavelengths of 394 and 464 nm, respectively.

The present study was supported by Grant-in-Aid for Scientific Research No. 21750207 from the Ministry of the Education, Culture, Sports, Science and Technology of Japan.

## References and Notes

- 1 K.-C. Park, H.-C. Ahn, H.-D. Nguyen, H.-Y. Jang, S.-I. Mho, *J. Korean Phys. Soc.* **2008**, *53*, 2220; Y. Tian, B. Chen, R. Hua, H. Zhong, L. Cheng, J. Sun, W. Lu, J. Wan, *Physica B* **2009**, *404*, 3598; J. Gu, Y. Zhu, H. Li, X. Zhang, Y. Qian, *J. Solid State Chem.* **2010**, *183*, 497.
- 2 S. Shi, X. Liu, J. Gao, J. Zhou, *Spectrochim. Acta, Part A* **2008**, *69*, 396.
- 3 G. J. McCarthy, R. D. Fischer, J. Sanzgeri, *J. Solid State Chem.* **1972**, *5*, 200; S. M. Kaczmarek, E. Tomaszewicz, D. Moszyński, A. Jasik, G. Leniec, *Mater. Chem. Phys.* **2010**, *124*, 646.
- 4 K. Koyabu, Y. Mayama, T. Masui, N. Imanaka, *J. Alloys Compd.* **2006**, *418*, 230; Y. Mayama, K. Koyabu, T. Masui, S. Tamura, N. Imanaka, *J. Alloys Compd.* **2006**, *418*, 243; S. W. Kim, T. Masui, H. Matsushita, N. Imanaka, *J. Electrochem. Soc.* **2010**, *157*, J181; S. W. Kim, K. Jyoko, T. Masui, N. Imanaka, *Materials* **2010**, *3*, 2506; S. W. Kim, K. Jyoko, T. Masui, N. Imanaka, *Chem. Lett.* **2010**, *39*, 604.
- 5 T. Honma, K. Toda, Z.-G. Ye, M. Sato, *J. Phys. Chem. Solids* **1998**, *59*, 1187.
- 6 Supporting Information is available electronically on the CSJ-Journal Web site, <http://www.csj.jp/journals/chem-lett/index.html>.
- 7 J. Wang, X. Jing, C. Yan, J. Lin, F. Liao, *J. Lumin.* **2006**, *121*, 57; Z. Wang, H. Liang, M. Gong, Q. Su, *Opt. Mater.* **2007**, *29*, 896.
- 8 R. D. Shannon, *Acta Crystallogr., Sect. A* **1976**, *32*, 751.
- 9 A. L. Allred, *J. Inorg. Nucl. Chem.* **1961**, *17*, 215.
- 10 O. A. Lopez, J. McKittrick, L. E. Shea, *J. Lumin.* **1997**, *71*, 1.
- 11 M. K. Chong, K. Pita, C. H. Kam, *Appl. Phys. A: Mater. Sci. Process.* **2004**, *79*, 433.
- 12 Z. Wang, H. Liang, M. Gong, Q. Su, *Electrochem. Solid-State Lett.* **2005**, *8*, H33.